AMERICAN SOCIETY FOR MICROBIOLOGY | Applied and Environmental Microbiology®

METHODS

Advanced Understanding of Prokaryotic Biofilm Formation through Use of a Cost-Effective and Versatile Multipanel Adhesion (mPAD) Mount

Stefan Schulze,[a] Heather Schiller,[a] Jordan Solomonic,[b] Orkan Telhan,[b] Kyle Costa,[c] Mechthild Pohlschroder[a]

[a]Department of Biology, University of Pennsylvania, Philadelphia, Pennsylvania, USA
[b]Weitzman School of Design, University of Pennsylvania, Philadelphia, Pennsylvania, USA
[c]Department of Plant and Microbial Biology, University of Minnesota, St. Paul, Minnesota, USA

Stefan Schulze and Heather Schiller contributed equally to this article. The author order was determined using an alternating author order for articles of both authors with equal contribution.

ABSTRACT Most microorganisms exist in biofilms, which comprise aggregates of cells surrounded by an extracellular matrix that provides protection from external stresses. Based on the conditions under which they form, biofilm structures vary in significant ways. For instance, biofilms that develop when microbes are incubated under static conditions differ from those formed when microbes encounter the shear forces of a flowing liquid. Moreover, biofilms develop dynamically over time. Here, we describe a cost-effective coverslip holder, printed with a three-dimensional (3D) printer, that facilitates surface adhesion assays under a broad range of standing and shaking culture conditions. This multipanel adhesion (mPAD) mount further allows cultures to be sampled at multiple time points, ensuring consistency and comparability between samples and enabling analyses of the dynamics of biofilm formation. As a proof of principle, using the mPAD mount for shaking, oxic cultures, we confirm previous flow chamber experiments showing that the *Pseudomonas aeruginosa* wild-type strain and a phenazine deletion mutant (Δ*phz*) strain form biofilms with similar structure but reduced density in the mutant strain. Extending this analysis to anoxic conditions, we reveal that microcolony formation and biofilm formation can only be observed under shaking conditions and are decreased in the Δ*phz* mutant compared to wild-type cultures, indicating that phenazines are crucial for the formation of biofilms if oxygen as an electron acceptor is unavailable. Furthermore, while the model archaeon *Haloferax volcanii* does not require archaella for surface attachment under static conditions, we demonstrate that an *H. volcanii* mutant that lacks archaella is impaired in early stages of biofilm formation under shaking conditions.

IMPORTANCE Due to the versatility of the mPAD mount, we anticipate that it will aid the analysis of biofilm formation in a broad range of bacteria and archaea. Thereby, it contributes to answering critical biological questions about the regulatory and structural components of biofilm formation and understanding this process in a wide array of environmental, biotechnological, and medical contexts.

KEYWORDS *Pseudomonas aeruginosa*, *Haloferax volcanii*, surface attachment, biofilms, biofilm assay, shear forces, *Archaea*, *Bacteria*, microcolonies

Planktonic prokaryotic cells often encounter highly stressful environmental conditions, such as those created by toxins or nutrient depletion. One strategy that bacteria and archaea have evolved to mitigate such stress is the establishment of a biofilm—a complex microbial community bound by a matrix of extracellular polymeric substances. The first steps in biofilm formation are cell adherence to a surface, quickly followed by cell

Editor Laura Villanueva, Royal Netherlands Institute for Sea Research

Address correspondence to Mechthild Pohlschroder, pohlschr@sas.upenn.edu.

The authors declare no conflict of interest.

Received 21 November 2021
Accepted 21 December 2021
Accepted manuscript posted online 5 January 2022
Published 22 February 2022

aggregation and microcolony formation; later, a mature biofilm is established. Adhesion often requires surface filaments (1–3). For example, *Pseudomonas aeruginosa*, a bacterium in which biofilm formation has been thoroughly studied, requires flagella and type IV pili to complete the initial steps of establishing a biofilm (4). For some organisms, additional components are also involved in biofilm maturation, such as redox-active secondary metabolites called phenazines. In *P. aeruginosa*, phenazines drive the release of extracellular DNA into the biofilm matrix and facilitate survival of cells in the anoxic core of a biofilm (5–7).

The large variety of platforms that have been developed to study biofilm formation seemingly reflect the diversity of attachment mechanisms and biofilm architectures that have evolved. While evolutionarily conserved type IV pili are required for surface adhesion in many organisms (8), as analyzed, e.g., through simple atmosphere-liquid interface (ALI) assays in standing cultures, the use of specific pilins can vary depending on the environmental conditions (2, 9, 10). Furthermore, while bacterial flagella and their archaeal counterparts (archaella) facilitate the binding to surfaces in some species (11), surface attachment in other species, like the model haloarchaeon *Haloferax volcanii*, appears to be independent of archaella (12). However, the involvement of type IV pili, archaella, and other cell surface structures in attachment and biofilm formation may depend on the environmental conditions under which ALI assays are performed. In fact, it has been shown that shear forces impact the ability of microbes to form biofilms, the characteristics of the established biofilms, and the rate of detachment in prokaryotic biofilms, e.g., for *Escherichia coli* (13, 14). Therefore, it is critical to analyze the formation of biofilms under various conditions, and more advanced platforms, such as complex flow chambers or rotating annular bioreactors, have been used for this task (15).

Despite the importance of generating data that will lead to critical discoveries about the molecular mechanisms that regulate the establishment of biofilms, each biofilm analysis method has intrinsic limitations. For instance, the standard ALI assay cannot be used to evaluate biofilm formation under flow (16) and thus prevents insight into the effect of shear forces on biofilm formation. Furthermore, this type of standing assay often allows undesirable liquid biofilm formation (17–19), making comparisons of planktonic and sessile cells unfeasible. As an alternative, some simple assays like the BioFilm Ring Test may be performed under shaking conditions, but this advantage comes with the drawback that microscopy cannot be used to analyze the biofilm (16). In contrast, more complex systems like flow chambers allow for detailed continuous imaging of biofilms (15, 20); however, it is extremely difficult to retrieve samples for molecular biological or biochemical evaluation at various time points. Some of these systems, including flow chambers and rotating annular bioreactors, are also costly (15). These limitations highlight that most biofilm analysis methods face a trade-off between high throughput and detail of analysis. High-throughput platforms like the standard ALI assay or BioFilm Ring Test only allow for rather superficial analyses of biofilm formation, while detailed analyses (e.g., in flow chambers) suffer from comparatively low throughput and limited versatility.

To overcome some of these challenges, we present a detailed description of the use of an inexpensive multipanel adhesion (mPAD) mount for the characterization of biofilm formation. This mount, which can be produced using a standard three-dimensional (3D) printer, facilitates the analysis of cell adhesion to coverslips for both standing and shaking cultures and under a variety of conditions. Using the mPAD mount, the same culture can be sampled at multiple time points for microscopic, biochemical, and molecular biological analyses.

As a proof of principle, we have analyzed *P. aeruginosa* biofilm formation under standing and shaking conditions, showing not only differences in biofilm architecture and the ability to proceed past the single-cell adhesion stage under anoxic conditions but also a decrease in microcolony formation in a phenazine knockout mutant (Δ*phz*) strain under shaking, anoxic conditions in contrast to wild-type cultures. Similarly, *H. volcanii* biofilms that formed in shaking cultures look very different from biofilms established

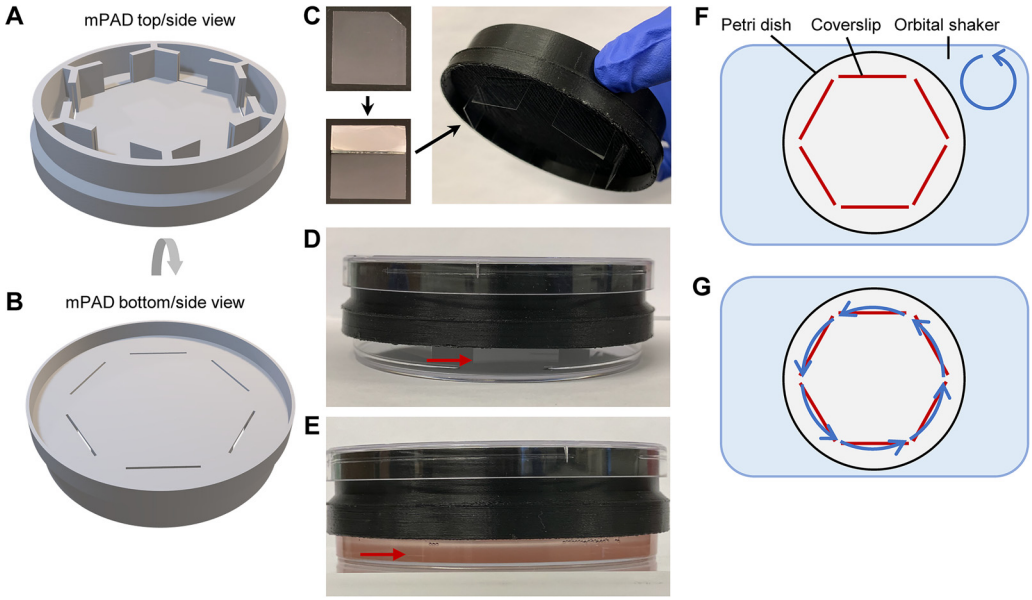

FIG 1 The 3D-printed mPAD mount can be used for biofilm assays under a broad range of conditions, including shaking. A 3D model of the mPAD mount is shown from the top/side view (A) and the bottom/side view (B). Coverslips can be inserted into the six slots at the bottom of the mPAD mount (C), and a piece of aluminum foil can be used to fit the coverslip more tightly (see Materials and Methods). Subsequently, the mPAD mount with inserted coverslips is placed onto a petri dish (D). After filling the petri dish with a cell culture (*H. volcanii* shown here), coverslips reach into the culture (E), allowing cells to adhere to the coverslip surface. The mPAD mount can be placed on an orbital shaker to expose cells to shear forces (F). The radial positioning of the slots of the mPAD mount ensures that cells adhering to any coverslip experience the same shear forces (G). Red arrows point to the lower end of inserted coverslips; blue arrows indicate shaking of the orbital shaker and the shear forces experienced by the coverslips.

in standing cultures, and we show that a strain lacking archaellins A1 and A2 (Δ*arlA1/2*) exhibits a decreased initial surface adhesion in shaking cultures despite lacking any defects under standing conditions, highlighting the importance of testing biofilm formation in wild-type and mutant strains under a variety of conditions.

RESULTS AND DISCUSSION

The mPAD mount is designed as a versatile and affordable device to characterize biofilm formation. Many invaluable tools have been developed over the past decades to characterize biofilm formation, ranging from simple ALI assays on coverslips in 12-well plates to sophisticated flow chambers that allow live observation of the stages of biofilm formation and comparison of various shear forces (15, 21). To combine the advantages of different types of assays, we designed the mPAD mount (Fig. 1). The costs of 3D printing the mPAD mount are relatively low (Table 1), similar to those of simple 12-well-plate assays, and the design of the mPAD mount to fit on standard petri dishes ensures its adaptability to different environmental conditions, including shear forces generated by constant shaking on an orbital shaker and an O_2-deprived atmosphere in an anaerobic chamber. Additionally, multiple slots within each mPAD mount enable the observation of different stages of biofilm formation by removing individual

TABLE 1 3D-printed mPAD mounts are affordable[a]

Material	Cost of material	Required amt of material per mPAD mount	Cost per mPAD mount
Formlabs High Temp resin	$200/L	70 mL (including support raft)	~$14
Monoprice PLA filament[b]	$20/kg	50 g (including support raft)	~$1

[a]The costs of 3D printing the mPAD mount depend on the material employed but are typically below $15 per mPAD mount. Furthermore, mPAD mounts can be reused without noticeable degradation over time.
[b]PLA, polylactic acid.

coverslips at different time points. This design also allows harvesting of samples for transcriptomics or proteomics analyses from different stages of biofilm formation from a single culture, thereby reducing high variabilities that can arise from the use of multiple cultures. Furthermore, shaking conditions prevent the formation of liquid biofilms. The resulting, more homogenous, planktonic phase aids in system-wide analyses comparing planktonic and sessile cells.

Radial positioning of the six slots of the mPAD mount ensures that all coverslips are exposed to the same shear forces when placed on an orbital shaker (Fig. 1F and G). With this design, only minimal differences between the inner and outer sides of the coverslip were observed (data not shown). However, due to the 3D printing of the mount, changes to the design are straightforward, and a variety of different layouts are conceivable, e.g., to increase the adhesion surface area or to accommodate movement of the liquid via a stirring bar instead of an orbital shaker (see Fig. S1 in the supplemental material).

3D printing of the mPAD furthermore supports a wide variety of materials, including materials that show high resistance to chemicals and temperature. In this study, we have used a Form 2 (Formlabs) 3D printer employing a High Temp resin (Formlabs) for the *P. aeruginosa* studies, as this material allows the mPAD mounts to be sterilized in an autoclave. For the biofilm studies of the archaeon *H. volcanii*, an MP Mini Delta 3D printer (Monoprice) using polylactic acid (PLA) filament (Monoprice) was employed to 3D print the mPAD mount. While PLA is not as resistant to heat and chemicals as Formlab's High Temp resin, it is more affordable (Table 1), and contamination of *H. volcanii* mid-log-phase cultures grown in medium containing ~2.5 M salt are very unlikely; thus, semisterile 70% ethanol washes could be employed instead of autoclaving. Notably, the material and sterilization technique used for the mPAD mount can be adapted freely by the user based on the organism and conditions to which the mPAD mount is applied.

The mPAD mount is suitable for characterization of *P. aeruginosa* wild-type and Δ*phz* mutant biofilms exposed to shear forces. The use of flow chambers has established that cell exposure to shear forces plays a significant role in the structure and architecture of *P. aeruginosa* biofilms (22, 23). Similarly, employing the mPAD mount setup on an orbital shaker facilitated the visualization of shear force effects on *P. aeruginosa* cultures because cells adhering to coverslips within this setup are experiencing shear forces from the moving liquid. For wild-type *P. aeruginosa* cultures, adhesion of individual cells to the coverslip after an hour was similar under shaking conditions to that under standing conditions using a common 12-well-plate ALI assay (Fig. 2). At 6 h, microcolonies were observed, and by 20 h, mature biofilms had formed under both conditions, but the biofilms formed under standing conditions were distributed more uniformly in a mixture of single cells, microcolonies, and large, three-dimensional biofilm structures. In contrast, under shaking conditions, cells formed large, dense, web-like structures with fewer visible unconnected microcolonies and single cells. The Δ*phz* strain showed a similar trend, although adhesion, microcolony formation, and mature biofilms were overall less dense than those of the wild type.

These results show that the mPAD mount is suitable for the analysis of different stages of biofilm formation under shaking conditions, with differences in biofilm architecture that are in line with previous experiments using flow chambers (6). For further analyses, cells can be washed off the coverslips (see below), e.g., to quantify adhesion through optical density at 600 nm (OD_{600}) measurements of crystal violet (24). Untreated adherent cells can also be retrieved (e.g., for omics experiments). Thereby, the mPAD mount sets the stage to compare the proteomes of biofilms formed under standing and shaking conditions to determine whether the differences are mainly structural or also include changes in the composition of the biofilm, including differentially expressed and posttranslationally modified proteins or differences in the exopolymeric substances.

Under anaerobic conditions, *P. aeruginosa* only forms microcolonies when exposed to shear forces. *P. aeruginosa* wild-type cultures can grow anaerobically, but comparisons of anaerobic biofilm formation with and without exposure to shear forces have thus far not been reported. In addition to characterizing wild-type biofilm formation under anaerobic, standing conditions, the versatility of the mPAD mount facilitated the analysis of shear

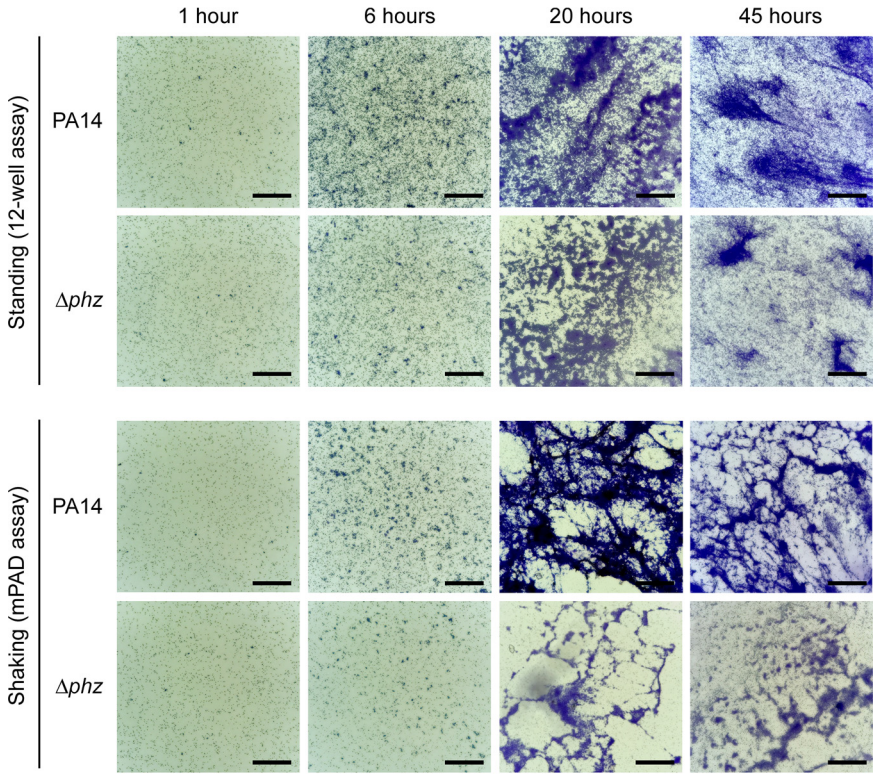

FIG 2 Using the mPAD mount for the analysis of *P. aeruginosa* biofilms under aerobic, shaking conditions confirmed that exposure to shear forces leads to different biofilm architectures and a noticeable phenotype in the Δ*phz* mutant. *P. aeruginosa* wild-type (PA14) and Δ*phz* mutant cultures were incubated under aerobic standing and shaking conditions for 1, 6, 20, and 45 h before staining of adherent cells with crystal violet. Images are representative of two biological replicates. The scale bar is 100 μm.

force impacts on surface attachment, microcolony formation, and biofilm formation under anaerobic conditions. Interestingly, while initial attachment to the coverslip occurred both with and without shaking, only cells exposed to shear forces through orbital shaking in the mPAD assay were able to form microcolonies and biofilms without available O_2, although these biofilms were significantly less dense than those under aerobic conditions (Fig. 3). Similar to the wild type, the Δ*phz* mutant was unable to form microcolonies under anaerobic, standing conditions. However, in comparison to the wild type, the adhesion and microcolony formation after 20 and 45 h under anaerobic, shaking conditions were reduced for the Δ*phz* strain and even lacking completely in one of the replicates. While this phenotype is similar to the reduced biofilm formation under aerobic conditions, the more pronounced effect under anaerobic conditions indicates a crucial role of phenazine as an electron acceptor when O_2 is not available. This role is in line with results on electron shuttling via phenazines in *P. aeruginosa* biofilms on agar plates (25).

***Haloferax volcanii* archaellins contribute to effective initial adhesion when exposed to shear forces.** While the haloarchaeon *H. volcanii* has been used as a model organism to study biofilm formation in archaea (17, 18, 26), to our knowledge, biofilm assays have not been performed under shaking conditions for any archaeon so far. Using the mPAD assay under shaking conditions, we could show that, similar to *P. aeruginosa*, *H. volcanii* can form biofilms under shaking conditions but exhibits distinct biofilm architectures dependent on the exposure to shear forces (Fig. 4). Under standing conditions, after 24 h, attachment of *H. volcanii* to the coverslip surface resulted in a dense layer of cells interspersed with areas of small microcolonies, which developed into larger areas of dense biofilms within 120 h. In contrast, under shaking conditions, *H. volcanii* attached only sparsely as single cells to the coverslip within 24 h, and some microcolonies formed as dense clusters of cells with network-like connections that

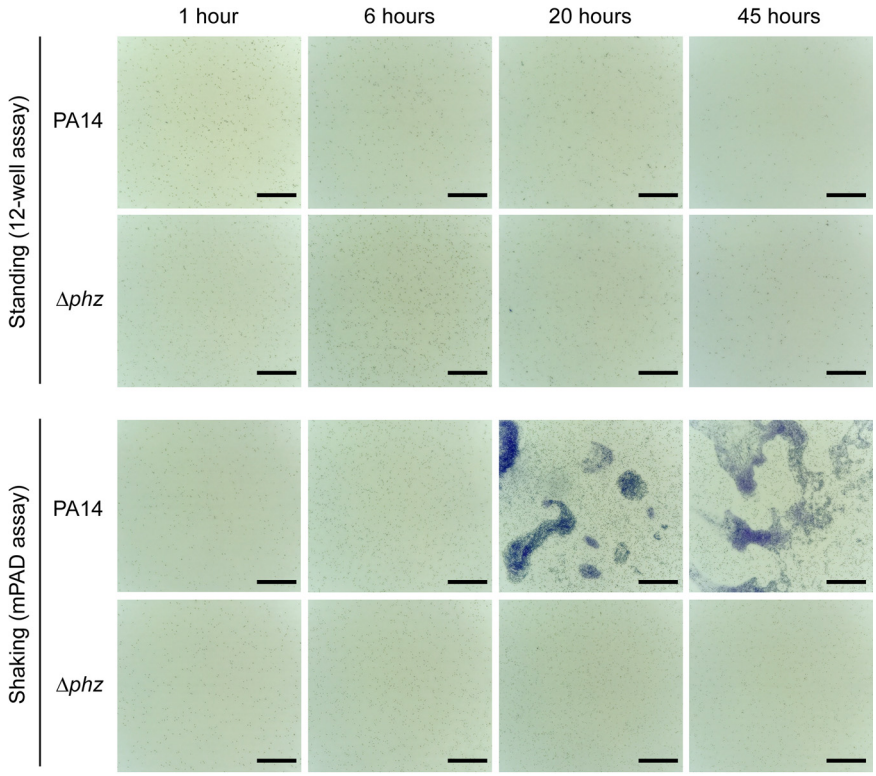

FIG 3 Employing the mPAD mount under anoxic conditions revealed that shear forces contribute to the formation of biofilms, which are dependent on *phz* under these conditions. *P. aeruginosa* wild-type (PA14) and Δ*phz* mutant cultures were incubated in an anaerobic chamber under standing and shaking conditions for 1, 6, 20, and 45 h before staining of adherent cells with crystal violet. Images are representative of two biological replicates. The scale bar is 100 μm.

likely consist of extracellular substances. After 120 h, these microcolonies grew into dense biofilm structures that were connected over larger areas.

The process of cell adhesion and microcolony formation without exposure to shear forces is independent of archaella in *H. volcanii*, as shown by the wild-type-like adhesion of a Δ*arlA1/2* mutant, which lacks both archaellins (12). This observation is in contrast to many bacteria and archaea, for which flagella and archaella, respectively, have been shown to be required for adhesion to surfaces (1, 27–30). To determine whether *H. volcanii* archaellins are required for biofilm formation when cells are exposed to shear forces, we compared the attachment of *H. volcanii* wild-type and Δ*arlA1/2* mutant cultures to coverslips under shaking conditions using the mPAD mount. At 120 h, both strains were able to form microcolonies and mature biofilm structures of similar magnitude and density (Fig. 4). However, at earlier stages, the mutant Δ*arlA1/2* strain did not adhere to the same extent as the wild type. While wild-type cultures at 24 h already formed microcolonies in addition to single-cell adhesion, the Δ*arlA1/2* strain exhibited mainly single-cell adhesion, and only a few, small clusters of cells were present.

Notably, the microscopically observed trends were confirmed through quantification of resolubilized crystal violet (Fig. 5). After 24 h under standing conditions, no quantitative difference in adhesion could be detected, while for the same time point under shaking conditions, the Δ*arlA1/2* mutant showed reduced adhesion. In contrast, while qualitative differences between the strains could not be observed through microscopy after 120 h, the Δ*arlA1/2* strain exhibited increased biofilm formation in the quantitative analysis under standing conditions but not under shaking conditions. Macroscopic images of the coverslips indicate that this quantitative difference may be due to an increased density of the biofilm at the ALI for the Δ*arlA1/2* mutant in comparison to the wild type (see Fig. S2

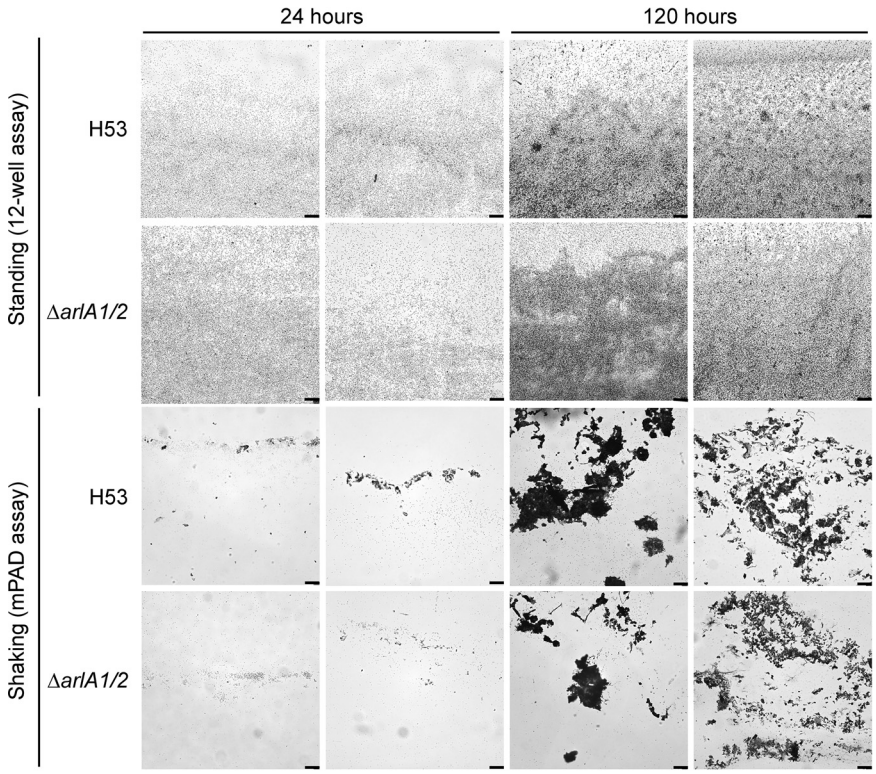

FIG 4 *H. volcanii* biofilm formation under shaking conditions differs substantially from that under standing conditions and is negatively affected by a lack of archaella. *H. volcanii* wild-type (H53) and Δ*arl1/2* mutant cultures were incubated under standing and shaking conditions at 45°C for 24 and 120 h before staining of adherent cells with crystal violet. Images are representative of two biological replicates. The scale bar is 50 μm.

in the supplemental material). Bright-field microscopy may not be suitable to detect this difference due to its limited ability to capture the three-dimensional depth of the biofilm.

Overall, these results indicate that archaella in *H. volcanii* could be involved in the initial surface attachment under shaking conditions. Possible explanations for a contribution of archaella in the binding to surfaces could be an increased sensing of the surface or movement toward it. Furthermore, the lack of archaella led to a denser biofilm

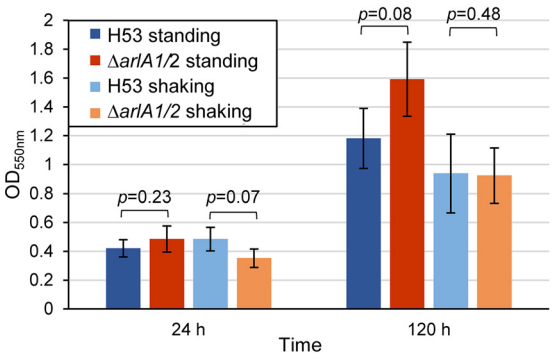

FIG 5 Quantification of biofilm formation confirms decreased surface adhesion of the *H. volcanii* Δ*arl1/2* mutant under shaking conditions. *H. volcanii* wild-type (H53) and Δ*arl1/2* cultures were incubated under standing and shaking conditions at 45°C for 24 and 120 h before staining of adherent cells with crystal violet. After staining, crystal violet was resolubilized and quantified via absorption at 550 nm in a 96-well plate reader. The height of the bars indicates the mean absorption of three biological replicates, while the error bar indicates the standard deviation of these replicates. A *t* test was performed comparing results for wild-type and mutant strains under standing and shaking conditions, and the resulting *P* values are shown.

under standing conditions after an extended incubation time (previous studies compared adhesion only after 24 h [12]), which may be the result of reduced biofilm dispersal due to nonmotile cells in the Δ*arlA1/2* mutant.

In general, in contrast to bacteria, the effects of shear forces on archaeal surface attachment and biofilm formation have not been analyzed so far. Our initial results here suggest that valuable insights into the molecular mechanisms of this process in archaea could be gained. The mPAD mount provides an ideal foundation for further studies because it can be used under a broad range of extreme conditions in which many model archaea thrive.

Conclusion. Biofilms represent the major life form of prokaryotes on Earth (31), and the conditions under which they occur are highly diverse and often not static. Therefore, we developed the simple, 3D-printed, versatile and affordable mPAD mount, which can be used to study prokaryotic biofilm formation under a wide variety of environmental conditions. The design of the mPAD mount thereby allows for samples to be taken from the same culture at multiple time points, capturing dynamic changes within the process of biofilm formation. This approach is well suited for subsequent microscopic as well as omics analyses: e.g., cells harvested from a single coverslip yield a total protein amount of around 10 μg, which is sufficient for proteomics analyses (see Table S1 in the supplemental material).

We could show the usefulness of the mPAD mount through the examples of *P. aeruginosa* and *H. volcanii* biofilm formation. For *P. aeruginosa*, we revealed that while biofilms do not form in the absence of O_2 under standing conditions, they can be observed when cultures are incubated under shaking conditions. It is likely that this increased biofilm formation under shaking conditions is the result of exposing cells to shear forces, since shear forces have previously been shown to contribute to *P. aeruginosa* biofilm formation under oxic conditions (22, 23). However, an increased nutrient availability under shaking conditions may contribute to this effect as well. Interestingly, *P. aeruginosa* Δ*phz* mutants are inhibited in their ability to form biofilms under anaerobic, shaking conditions. For *H. volcanii*, we could reveal that biofilms can form under shaking conditions and exhibit a different biofilm architecture than under standing conditions. Additionally, *H. volcanii* archaella seem to be involved in the initial surface adhesion under shaking, but not under standing, conditions. These results show not only the biological insights that can be gained from biofilm assays under a variety of conditions but also highlight the versatility of the mPAD mount. With the increased availability of 3D printing capabilities and the straightforward changes that can be made to the design of the mPAD mount, the range of applications will widen even further.

MATERIALS AND METHODS

Strains and growth conditions. *P. aeruginosa* PA14 and the *P. aeruginosa* Δ*phz* mutant (32) were grown at 37°C in lysogeny broth (Difco) in culture tubes (18 by 150 mm) under shaking conditions (orbital shaker at 250 rpm, 1-in. orbital diameter), if not specified otherwise. For anaerobic growth, 40 mM sodium nitrate (Fisher Science Education) and 200 mM MOPS (morpholinepropanesulfonic acid) (Fisher Bioreagents) were included in the medium, and cultures were grown standing inside a heated (37°C) Coy-type anoxic chamber with an atmosphere of 2 to 3% H_2, 10% CO_2, and balance N_2. MOPS buffer was included to avoid pH changes from reduction of nitrate and the high-CO_2 atmosphere in the chamber. For growth as a biofilm, overnight cultures were subinoculated (50× dilution), grown for several hours to an OD_{600} between 1.0 and 1.5, and then further diluted to an OD_{600} of 0.3. These cultures were immediately transferred to biofilm growth conditions by incubating them either standing in 12-well plates or shaking in petri dishes (Fisherbrand; 100 mm by 15 mm) with the mPAD mount (see below).

H. volcanii H53 and the *H. volcanii* Δ*arlA1/2* mutant (12) were grown at 45°C in liquid (orbital shaker at 250 rpm, 1-in. orbital diameter) or on solid agar (containing 1.5% [wt/vol] agar) semidefined Casamino Acids (Hv-Cab) medium (33), supplemented with tryptophan (+Trp) (Fisher Scientific) and uracil (+Ura) (Sigma) at a final concentration of 50 μg mL^{-1}. A colony from a solid Hv-Cab plate (incubated for 3 to 5 days at 45°C) was inoculated into 5 mL Hv-Cab liquid medium (16-mm culture tube diameter). After incubating the culture tubes overnight at 45°C with shaking (orbital shaker at 250 rpm, 1-in. orbital diameter) until the strains reached mid-log phase (OD_{600} of ~0.7), the strains were diluted to an OD_{600} of 0.01 into a final volume of 20 mL (24-mm culture tube diameter), followed by incubation at 45°C with shaking (orbital shaker at 250 rpm, 1-in. orbital diameter) until cultures reached an OD_{600} of 0.35. Each culture was then transferred into either a 12-well plate or a sterile plastic petri dish (Fisherbrand; 100 mm by 15 mm) for biofilm growth conditions (see below).

Printing of mPAD mount. The 3D model of the mPAD mount can be downloaded from Thingiverse (https://www.thingiverse.com/thing:4784964). A Form 2 (Formlabs) 3D printer using High Temp resin (V2; Formlabs) was used to print mPAD mounts that can be sterilized in an autoclave. The printing resolution (layer height) was 50 μm. After printing, the curing procedure consisted of a 6-min wash in 90% isopropanol, followed by incubation for 2 h at 80°C. These mounts were used for the *P. aeruginosa* biofilm assays. Conversely, an MP Mini Delta 3D printer (Monoprice) using polylactic acid (PLA) filament (Monoprice) was employed to 3D print the mPAD mounts used for assays with *H. volcanii*.

Setting up the mPAD mount for adhesion assays under standing and shaking conditions. (i) *P. aeruginosa* biofilms. For *P. aeruginosa* biofilms, glass coverslips (22 mm by 22 mm by 1.5 mm; Fisher Scientific) were marked to be able to distinguish the two sides (facing inward and outward from the mPAD mount), as well as the top and bottom of the coverslip. When inserting the coverslips into the mPAD mount, thin pieces of aluminum foil were placed at the top of the coverslip to enable a tighter fit. Since the accuracy of the 3D printing varies slightly, coverslips may fit only loosely into the slots of the mPAD mount. The aluminum foil provides additional thickness at the top of the coverslip, thereby enabling a tighter fit into the mPAD mount and preventing the risk of coverslips falling out of their slots during shaking incubation. Assembled mPAD mounts were autoclaved to sterilize all surfaces. *P. aeruginosa* culture (grown and diluted as described above) was placed in the bottom half of an empty petri dish, and the mPAD mount was placed on top of the petri dish, with each coverslip reaching at least 0.5 cm into the culture. The petri dish lid was placed on top of the mPAD mount before incubating the assembled setup in a humidified chamber at 37°C. Cell attachment was allowed to occur for 30 min before placing the chamber on an orbital shaker set to 60 rpm. For static biofilms, 2 mL of culture at an OD_{600} of 0.3 was aliquoted into a 12-well plate (Falcon) with a glass coverslip standing upright (perpendicular to the bottom of the well) in each well. Both wild-type and Δ*phz* mutant biofilms were grown via the methods described above under both oxic and anoxic conditions.

(ii) *H. volcanii* biofilms. For *H. volcanii* biofilms, mPAD mounts were washed with 70% ethanol and allowed to air dry before insertion of the marked coverslips (described above) into the slits of the mPAD mount. Thin pieces of autoclaved aluminum foil were placed at the top of the coverslip to enable a tighter fit in the mPAD mount. The mPAD mount with inserted coverslips was placed onto the bottom half of the petri dish containing the liquid culture, with each coverslip reaching at least 0.5 cm into the culture. The petri dish lid was placed on top of the mPAD mount before placing the petri dish with the mPAD mount into a humidified chamber. The cultures were incubated at 45°C on an orbital shaker (0.75-in. orbital diameter) set to 60 rpm. For static biofilms, 2 mL of *H. volcanii* culture at an OD_{600} of 0.35 was aliquoted into a 12-well plate (Falcon) with a glass coverslip standing upright in each well. Both wild-type and Δ*arlA1/2* mutant biofilms were grown via the methods described above under oxic conditions.

Staining and imaging. (i) *P. aeruginosa* biofilms. For *P. aeruginosa* biofilms, coverslips were removed at 1, 6, 20, and 45 h, submerged briefly in 0.5% NaCl to wash off loosely attached cells, and fixed by placing the coverslip in 3 mL of a 0.5% NaCl–2% glutaraldehyde solution in a 12-well plate for 30 min at room temperature. For anaerobically grown cultures, the fixation step was performed inside the anoxic chamber before moving the coverslips into an oxic atmosphere for further processing. After fixation, the coverslips were immediately placed into 3 mL of 0.1% crystal violet for 10 min. After staining, coverslips were washed in H_2O and allowed to dry before imaging. Coverslips were imaged on an ECHO Revolve R4 hybrid microscope with a universal slide mount. The microscope was operated in the upright orientation with an extra-long-working-distance condenser (NA, 0.30; working distance, 73 mm). Images were taken with either a 20× fluorite (NA, 0.45; working distance, 6.6 to 7.8 mm) or 40× fluorite (NA, 0.75; working distance, 0.51 mm) lens objective, using an iPAD (iPad Pro, 2nd generation) camera for image acquisition. Images were collected from the middle of the slide near the location of the ALI.

(ii) *H. volcanii* biofilms. For *H. volcanii* biofilms, coverslips were removed at 24 and 120 h, submerged briefly in 18% saltwater (33), and fixed by placing them in 2% acetic acid (Acros Organics) in small petri dishes (Corning; 35 mm by 10 mm) for 10 min at room temperature. After fixation, the coverslips were allowed to air dry. Cells attached to coverslips were stained by submerging them into 0.1% crystal violet (Acros) for 10 min. After removing the coverslips from the crystal violet solution, they were rinsed twice with H_2O and air dried. Biofilms were imaged using a DMi8 inverted microscope with bright-field settings using 20× PL Fluotar (NA, 0.55; working distance, 1.2 mm) and 40× PL Fluotar (NA, 0.6; working distance, 3.3 to 1.9) objectives, an attached Leica DFC9000 GT camera, and the Leica Application Suite X (version 3.6.0.20104) software. Representative images were collected across the width of the coverslip (excluding the edges) near the location of the ALI.

Quantification of crystal violet. After staining of coverslips, crystal violet was resolubilized by rinsing coverslips two times with 100 μL of 30% acetic acid. Using a pipette, the acetic acid solution was repeatedly rinsed over the stained coverslip until all crystal violet was resolubilized. During this process, the solution was collected in a small petri dish, and after each resolubilization step, the crystal violet-containing solution was transferred into a well of a 96-well plate (pooling the solution of both rinses). The resolubilized crystal violet from samples taken after 120 h was diluted 1:1 in 30% acetic acid. The OD_{550} was measured using a 96-well plate reader (BioTek PowerWave XS2). Quantification was performed for three biological replicates, and the resulting values for wild-type and mutant strains under standing and shaking conditions were compared using a two-sample *t* test assuming equal variance (Microsoft Excel).

Quantification of protein amounts. In order to harvest adherent cells from coverslips under shaking conditions, coverslips were rinsed with 750 μL H_2O, followed by 500 μL 1% SDS, followed by 500 μL H_2O. At each step, the solution was repeatedly rinsed over the coverslip using a pipette, and the solution was collected in a small petri dish before transferring it to a 2-mL tube. The protein-containing cell lysate

was concentrated to 100 μL in 0.5-mL filter units (Millipore) via centrifugation at 14,000 $\times$ *g*. The protein concentration of the concentrate was determined using a bicinchoninic acid (BCA) assay kit (Pierce, Thermo Fisher) following manufacturer's instructions and measuring absorption at 562 nm in a 96-well plate reader (BioTek PowerWave XS2).

SUPPLEMENTAL MATERIAL

Supplemental material is available online only.

SUPPLEMENTAL FILE 1, PDF file, 0.5 MB.

ACKNOWLEDGMENTS

We thank the University of Pennsylvania Libraries' Biotech Commons for courtesy 3D printing of mPAD mounts.

S.S., H.S., and M.P. acknowledge support from National Science Foundation Grant 1817518. K.C. acknowledges support from a Young Investigator Award from the Army Research Office (grant no. W911NF-19-1-0024).

We declare no conflict of interest.

REFERENCES

1. van Wolferen M, Orell A, Albers S-V. 2018. Archaeal biofilm formation. Nat Rev Microbiol 16:699–713. https://doi.org/10.1038/s41579-018-0058-4.
2. Pohlschroder M, Esquivel RN. 2015. Archaeal type IV pili and their involvement in biofilm formation. Front Microbiol 6:190. https://doi.org/10.3389/fmicb.2015.00190.
3. Chaudhury P, Quax TEF, Albers S-V. 2018. Versatile cell surface structures of archaea: cell surface structures of archaea. Mol Microbiol 107:298–311. https://doi.org/10.1111/mmi.13889.
4. O'Toole GA, Kolter R. 1998. Flagellar and twitching motility are necessary for *Pseudomonas aeruginosa* biofilm development. Mol Microbiol 30:295–304. https://doi.org/10.1046/j.1365-2958.1998.01062.x.
5. Glasser NR, Kern SE, Newman DK. 2014. Phenazine redox cycling enhances anaerobic survival in *P seudomonas aeruginosa* by facilitating generation of ATP and a proton-motive force: phenazines facilitate energy generation. Mol Microbiol 92:399–412. https://doi.org/10.1111/mmi.12566.
6. Ramos I, Dietrich LEP, Price-Whelan A, Newman DK. 2010. Phenazines affect biofilm formation by Pseudomonas aeruginosa in similar ways at various scales. Res Microbiol 161:187–191. https://doi.org/10.1016/j.resmic.2010.01.003.
7. Saunders SH, Tse ECM, Yates MD, Otero FJ, Trammell SA, Stemp EDA, Barton JK, Tender LM, Newman DK. 2020. Extracellular DNA promotes efficient extracellular electron transfer by pyocyanin in Pseudomonas aeruginosa biofilms. Cell 182:919–932.e19. https://doi.org/10.1016/j.cell.2020.07.006.
8. Berry J-L, Pelicic V. 2015. Exceptionally widespread nanomachines composed of type IV pilins: the prokaryotic Swiss Army knives. FEMS Microbiol Rev 39:134–154. https://doi.org/10.1093/femsre/fuu001.
9. Legerme G, Pohlschroder M. 2019. Limited cross-complementation between Haloferax volcanii PilB1-C1 and PilB3-C3 paralogs. Front Microbiol 10:700. https://doi.org/10.3389/fmicb.2019.00700.
10. Hsiao A, Toscano K, Zhu J. 2008. Post-transcriptional cross-talk between pro- and anti-colonization pili biosynthesis systems in Vibrio cholerae: pili biosynthesis systems in Vibrio cholerae. Mol Microbiol 67:849–860. https://doi.org/10.1111/j.1365-2958.2007.06091.x.
11. Jarrell K, Ding Y, Nair D, Siu S. 2013. Surface appendages of Archaea: structure, function, genetics and assembly. Life (Basel) 3:86–117. https://doi.org/10.3390/life3010086.
12. Tripepi M, Imam S, Pohlschröder M. 2010. Haloferax volcanii flagella are required for motility but are not involved in PibD-dependent surface adhesion. J Bacteriol 192:3093–3102. https://doi.org/10.1128/JB.00133-10.
13. Fink R, Oder M, Rangus D, Raspor P, Bohinc K. 2015. Microbial adhesion capacity. Influence of shear and temperature stress. Int J Environ Health Res 25:656–669. https://doi.org/10.1080/09603123.2015.1007840.
14. Alsharif G, Ahmad S, Islam MS, Shah R, Busby SJ, Krachler AM. 2015. Host attachment and fluid shear are integrated into a mechanical signal regulating virulence in Escherichia coli O157:H7. Proc Natl Acad Sci U S A 112:5503–5508. https://doi.org/10.1073/pnas.1422986112.
15. Azeredo J, Azevedo NF, Briandet R, Cerca N, Coenye T, Costa AR, Desvaux M, Di Bonaventura G, Hébraud M, Jaglic Z, Kačániová M, Knøchel S, Lourenço A, Mergulhão F, Meyer RL, Nychas G, Simões M, Tresse O, Sternberg C. 2017. Critical review on biofilm methods. Crit Rev Microbiol 43:313–351. https://doi.org/10.1080/1040841X.2016.1208146.
16. Magana M, Sereti C, Ioannidis A, Mitchell CA, Ball AR, Magiorkinis E, Chatzipanagiotou S, Hamblin MR, Hadjifrangiskou M, Tegos GP. 2018. Options and limitations in clinical investigation of bacterial biofilms. Clin Microbiol Rev 31:e00084-16. https://doi.org/10.1128/CMR.00084-16.
17. Chimileski S, Franklin MJ, Papke RT. 2014. Biofilms formed by the archaeon Haloferax volcanii exhibit cellular differentiation and social motility, and facilitate horizontal gene transfer. BMC Biol 12:65. https://doi.org/10.1186/s12915-014-0065-5.
18. Schiller H, Schulze S, Mutan Z, de Vaulx C, Runcie C, Schwartz J, Rados T, Bisson Filho AW, Pohlschroder M. 2020. Haloferax volcanii immersed liquid biofilms develop independently of known biofilm machineries and exhibit rapid honeycomb pattern formation. mSphere 5:e00976-20. https://doi.org/10.1128/mSphere.00976-20.
19. Armitano J, Méjean V, Jourlin-Castelli C. 2014. Gram-negative bacteria can also form pellicles: floating biofilm in Gram-negative bacteria. Environ Microbiol Rep 6:534–544. https://doi.org/10.1111/1758-2229.12171.
20. Blanco-Cabra N, López-Martínez MJ, Arévalo-Jaimes BV, Martin-Gómez MT, Samitier J, Torrents E. 2021. A new BiofilmChip device for testing biofilm formation and antibiotic susceptibility. NPJ Biofilms Microbiomes 7:62. https://doi.org/10.1038/s41522-021-00236-1.
21. Gomes LC, Mergulhão FJM. 2021. A selection of platforms to evaluate surface adhesion and biofilm formation in controlled hydrodynamic conditions. Microorganisms 9:1993. https://doi.org/10.3390/microorganisms9091993.
22. Mordue J, O'Boyle N, Gadegaard N, Roe AJ. 2021. The force awakens: the dark side of mechanosensing in bacterial pathogens. Cell Signal 78:109867. https://doi.org/10.1016/j.cellsig.2020.109867.
23. Rodesney CA, Roman B, Dhamani N, Cooley BJ, Katira P, Touhami A, Gordon VD. 2017. Mechanosensing of shear by Pseudomonas aeruginosa leads to increased levels of the cyclic-di-GMP signal initiating biofilm development. Proc Natl Acad Sci U S A 114:5906–5911. https://doi.org/10.1073/pnas.1703255114.
24. Kwasny SM, Opperman TJ. 2010. Static biofilm cultures of Gram-positive pathogens grown in a microtiter format used for anti-biofilm drug discovery. Curr Protoc Pharmacol 50:13A.8.1–13A.8.23.
25. Schiessl KT, Hu F, Jo J, Nazia SZ, Wang B, Price-Whelan A, Min W, Dietrich LEP. 2019. Phenazine production promotes antibiotic tolerance and metabolic heterogeneity in Pseudomonas aeruginosa biofilms. Nat Commun 10:762. https://doi.org/10.1038/s41467-019-08733-w.
26. Esquivel RN, Schulze S, Xu R, Hippler M, Pohlschroder M. 2016. Identification of *Haloferax volcanii* pilin N-glycans with diverse roles in pilus biosynthesis, adhesion, and microcolony formation. J Biol Chem 291:10602–10614. https://doi.org/10.1074/jbc.M115.693556.
27. Holten MP, Fonseca DR, Costa KC. 2021. The oligosaccharyltransferase AglB supports surface-associated growth and iron oxidation in Methanococcus maripaludis. Appl Environ Microbiol 87:e00995-21. https://doi.org/10.1128/AEM.00995-21.
28. Jarrell KF, Stark M, Nair DB, Chong JPJ. 2011. Flagella and pili are both necessary for efficient attachment of Methanococcus maripaludis to surfaces: flagella and pili necessary for M. maripaludis attachment. FEMS Microbiol Lett 319:44–50. https://doi.org/10.1111/j.1574-6968.2011.02264.x.

29. Haiko J, Westerlund-Wikström B. 2013. The role of the bacterial flagellum in adhesion and virulence. Biology (Basel) 2:1242–1267. https://doi.org/10.3390/biology2041242.
30. Belas R. 2014. Biofilms, flagella, and mechanosensing of surfaces by bacteria. Trends Microbiol 22:517–527. https://doi.org/10.1016/j.tim.2014.05.002.
31. Flemming H-C, Wuertz S. 2019. Bacteria and archaea on Earth and their abundance in biofilms. Nat Rev Microbiol 17:247–260. https://doi.org/10.1038/s41579-019-0158-9.
32. Dietrich LEP, Price-Whelan A, Petersen A, Whiteley M, Newman DK. 2006. The phenazine pyocyanin is a terminal signalling factor in the quorum sensing network of Pseudomonas aeruginosa. Mol Microbiol 61:1308–1321. https://doi.org/10.1111/j.1365-2958.2006.05306.x.
33. de Silva RT, Abdul-Halim MF, Pittrich DA, Brown HJ, Pohlschroder M, Duggin IG. 2021. Improved growth and morphological plasticity of Haloferax volcanii. Microbiology 167 https://doi.org/10.1099/mic.0.001012.